In vitro evaluation of TiO2 nanotubes as cefuroxime carriers on orthopaedic implants for the prevention of periprosthetic joint infections

P. Chennell, E. Feschet-Chassot, T. Devers, K.O. Awitor, S. Descamps, V. Sautou

In-vitro evaluation of TiO_2 nanotubes as cefuroxime carriers on orthopedic implants for the prevention of periprosthetic joint infections

Structured Abstract:

Context: The prevention of periprosthetic joint infections requires an antibiotic prophylactic therapy, which could be delivered locally using titanium dioxide nanotubes as novel reservoirs created directly on the orthopaedic implant titanium surface.

Objective: In this study, the influence of several parameters that could impact the use of titanium dioxide nanotubes as cefuroxime carriers was investigated.

Method: Cefuroxime loading and release was studied for 90 minutes with three nano-topography conditions (nano-smooth, nano-rugged and nano-tubular), two cefuroxime loading solution concentrations (150 mg/mL and 25 mg/mL) and two nano-tubular crystalline structures.

Results: In all tested conditions, maximum amount of cefuroxime was obtained within two minutes. For both cefuroxime loading solution concentrations, nano-smooth samples released the least cefuroxime, and the nano-tubular samples released the most, and a six-fold increase in the concentration of the cefuroxime loading increased the amount of cefuroxime quantified by more than seven times, for all tested nano-topographies. However, the nano-tubes' crystalline structure did not have any influence on the amount of cefuroxime quantified.

Conclusion: The results demonstrated that the surface nano-topography and loading solution concentration influence the efficiency of titanium dioxide nanotubes as cefuroxime carriers and need to be optimized for use as novel reservoirs for local delivery of cefuroxime to prevent periprosthetic infections.

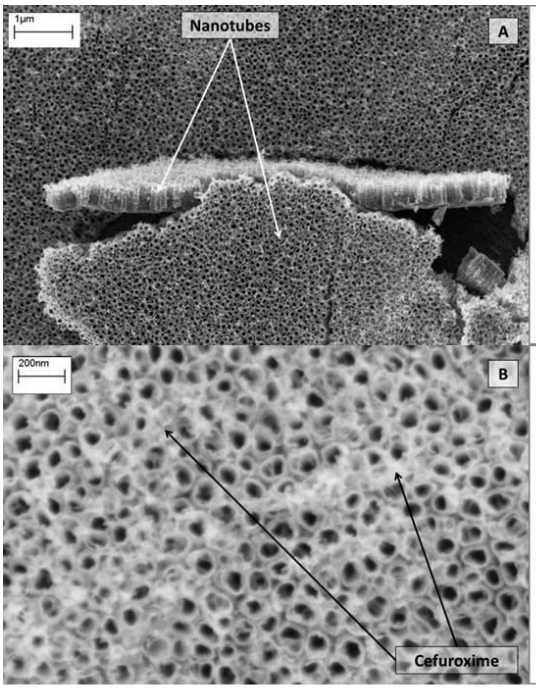

Surface topography of a nano-tubular anodized TiO_2 sample by SEM, before loading (A) and after loading with cefuroxime deposit and infiltration in the surface nanopores (B)

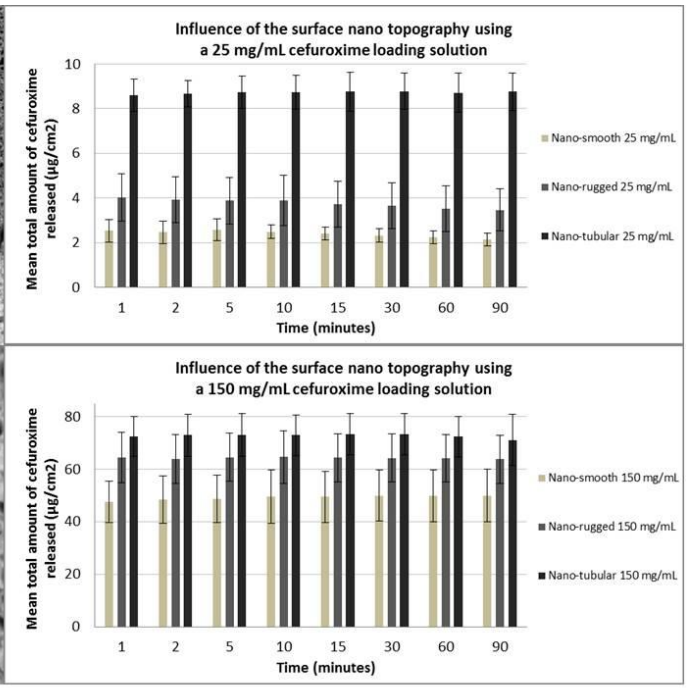

Total amount of released cefuroxime during 90 minutes for the different tested nano-topography and cefuroxime loading solution conditions

29

30

In-vitro evaluation of TiO_2 nanotubes as cefuroxime carriers on orthopedic implants for the prevention of periprosthetic joint infections

P. Chennell[1,2], E. Fechet-Chassot[1], T. Devers[3], K.O. Awitor[1], S. Descamps[1,4], V. Sautou[1,2]

[1] EA 4676 C-BIOSENSS, Clermont Université, Université d'Auvergne, BP 10448, F-63000 Clermont-Ferrand, France

[2] Service Pharmacie, CHU Clermont-Ferrand, F-63003 Clermont-Ferrand, France

[3] FRE 3520, CNRS - Université d'Orléans, 1b rue de la férollerie, 45071 Orléans Cedex 2, France

[4] Service de Chirurgie Orthopédique, CHU Clermont-Ferand, F-63003 Clermont-Ferrand, France

Corresponding author :

Philip Chennell

pchennell@chu-clermontferrand.fr

C-BIOSENSS, 4th R2, Faculty of Medicine and Pharmacy, Place Henri Dunant, 63000 Clermont-Ferrand cedex, France

Mobile : +33(0)6.38.13.79.11

Keywords:

Periprosthetic joint infections, Drug delivery systems, Titanium dioxide, Nanotubes, Cefuroxime

Introduction

Total knee and hip arthroplasties (TKA and THA) are frequent orthopaedic procedures, with over 4,400,000 TKA and 2,100,000 THA having been performed

between 1998 and 2008 in the United States (Memtsoudis et al., 2012). Periprosthetic joint infection incidences vary notably with patient comorbidities, but are estimated to range between 0.86% to 1.1% for TKA and between 0.3% to 1.63% for THA (Dale et al., 2011; Jämsen et al., 2010; Ong et al., 2009; Phillips, 2006; Pulido et al., 2008). With the number of TKA and THA predicted to grow by nearly 600% and more than 100% respectively between 2005 and 2030 in the United States (S. Kurtz et al., 2007; Iorio et al., 2008), the absolute number of periprosthetic joint infections is set to increase. The most prevalent etiological agents of orthopaedic infections are gram positive opportunistic cocci, namely *Staphylococcus aureus* and *Staphylococcus* epidermidis, responsible for more than two thirds of all infections (Campoccia et al., 2006; Montanaro et al., 2011). If surgical debridement combined with antibiotic therapy and implant retention is still possible in the early stages of infections, in the other cases a surgical revision with implant ablation and several weeks of intravenous antibiotic therapy is necessary to treat the infection completely (Cuckler, 2005; Senthi et al., 2011).

A prophylactic systemic antibiotic treatment is recommended when using implantable medical devices such as articular implants (AlBuhairan et al., 2008; Meehan et al., 2009; Kuong et al., 2009; Gillespie and Walenkamp, 1996; Société de Pathologie Infectieuse de Langue Française (SPILF), 2009). Regrettably, due to the disturbed bone structure and local vascularity, caused by the trauma of the surgery, as well as probable initial bad distribution of antibiotics into the bone (Smilack et al., 1976), it is thought that the achieved *in situ* concentrations might not be enough to exceed minimal inhibition concentrations (Schmidmaier et al., 2006; Zilberman and Elsner, 2008), leading to a suboptimal efficiency.

Recently, the use of self-assembled titanium dioxide nanotubes (TiO_2 NT) as reservoirs for localized antibiotic prophylactic therapy has been described (Ayon et al., 2006; Gulati et al., 2011; Kang et al., 2007; Losic and Simovic, 2009; Macak et al., 2007; Popat et al., 2007). Created directly on the titanium surface, TiO_2 NT, in certain conditions, have been shown to improve osteoblast adhesion, reduce bacterial colonization and serve as a reservoir for drugs (Losic and Simovic, 2009; Gulati et al., 2011; Ghicov and Schmuki, 2009; Roy et al., 2011), possibly allowing an *in situ* release of antibiotics after the prosthesis implantation.

In this work, Cefuroxime, a second generation cephalosporin, was chosen as a model drug as its use is recommended by the American Academy of Orthopaedic surgeons (Meehan et al., 2009) and by the French Society of Anaesthesia and Intensive care (Société française d'anesthésie et de réanimation, 2011) for antibiotic prophylactic treatment in orthopaedic surgery. Moreover, to our knowledge, there is no data in the literature concerning the use of nanotubes as cefuroxime carriers.

We studied the influence of several parameters that could have an impact on the use of TiO_2 NT as a cefuroxime carrier: the surface nano-topography (smooth versus nano-rugged versus nanostructured titanium samples), the loading solution concentration (by comparing the use of a saturated solution of cefuroxime (150 mg/mL) to a much lesser concentrated solution (25 mg/mL), for each nano-topography condition) and the nanotube's crystalline structure (annealed nanotubes versus non-annealed nanotubes).

I. Materials and methods

A. Sample preparation

1. Titanium samples

Unpolished titanium foil (99.6% purity, 0.1 mm thickness, Goodfellow, Lille France) was first cut into rectangular samples (2.5 X 1.5 cm), which were then degreased by successive 5 minutes sonications in trichloroethylene (VWR BDH Prolabo, Fontenay-sous-Bois, France), acetone (Merck Millipore, Darmstadt, Germany) and methanol (UCB Pharma France, Colombes, France), then rinsed with deionised water, dried in the oven at 100 °C and finally cooled in a desiccator. The obtained samples are later on referred to as nano-smooth samples.

To obtain nano-rugged surfaces, but without fully formed nanotubes, the as previously described cleaned titanium foil samples (smooth samples) were anodized by immersion to a height of 1.5 cm in a 0.4 wt. % HF aqueous solution with a platinium cathode, as schematized in Figure 1. The anodizing voltage was maintained at 20 V, for 80 seconds, at a constant temperature of 20 °C.

To obtain TiO_2 nanotubes (nano-tubular samples), the anodization was carried out in the same conditions as described above but for 20 minutes.

All experiments were conducted on the obtained nano-smooth, nano-rugged or nano-tubular titanium foil.

To convert the amorphous nanotubes into the mixed crystalline phases of anatase and rutile, some samples were annealed at 500°C for 2 hours under oxygen, with a heating and cooling rate of 5 °C min^{-1}.

2. Cefuroxime loading solutions

A 150 mg/mL cefuroxime solution was prepared by dissolving 1.5 g of cefuroxime (Panpharma, Fougeres, France, batch No 104179) with sterile deionised water (VERSYLENE®, Fresenius Kabi, Louviers, France) to a total volume of 10 mL.

3. Loading method and storage

To load the samples with cefuroxime, an adapted soaking technique was used (Ayon et al., 2006; Kim et al., 2008). Each sample was immersed to a height of 1.5 cm, in either a 150 mg/ml or a 25 mg/mL solution of cefuroxime, for 30 minutes, in ambient daylight, at room temperature (22-26°C). At the end of the loading time, the samples were removed from the immersion solution and were immediately air blown to remove excess solution on the surface and to dry them.

The samples were stored prior to loading and after loading, until cefuroxime quantification, in a climate chamber (BINDER GmbH, Tuttlingen, Germany), in the dark, at 25°C.

B. Sample characterizations

1. Structural characterizations

The crystalline structure and phase of the TiO_2 nanotube layers of a smooth, a non-annealed and an annealed nano-tubular sample were determined by X-ray diffraction

(XRD) using a Scintag XRD X'TRA diffractometer with CuKα (λ = 1.54° radiation). The CuK_{β} radiation was filtered through a nickel filter. The diffraction pattern was achieved between 20 and 80◦ with a step angle of 0.05° and a scanning speed of 0.01° per second.

For the study of the surface nano-topography, structural characterization of a smooth, a nano-rugged and a nano-tubular sample was performed before and after drug loading with two different concentration cefuroxime solutions using a field emission scanning electron microscope (SEM). It was performed using a Supra 55 VP SEM (Carl Zeiss SMT, Nanterre, France) with secondary emission and in lens detector. The accelerating voltage and the working distance were respectively 3 kV and either 5 or 6 mm (image dependent).

Images were acquired at different scan sizes from the top surface.

For the four different tested conditions of titanium foil nano-topography and crystalline structure (smooth, nano-rugged, non-annealed nano-tubular and annealed nano-tubular), surface wettability was investigated using a drop shape analysis system (EasyDrop, Kruss, Hamburg, Germany). The contact angle was measured with a deionized water sensile droplet of 3 µL in ambient conditions. The measurement was taken 5 seconds after the deposition of the water droplet on the substrate. After measurement, the samples were cleaned, dried in nitrogen and stored in a desiccator.

2. Cefuroxime quantification

Each sample was placed into a known volume of sterile deionised water (5 or 10 mL depending on the estimated loaded quantity of cefuroxime), for 90 minutes. At determined times (1; 2; 5; 10; 15; 30; 60 and 90 minutes) a determined volume (1000 µL) of release solution was collected and was replaced with the same volume of fresh sterile deionised water.

The cefuroxime present in the collected sample was then quantified by HPLC composed of a PU-2080 Plus pump, and an AS-2055 Plus auto-sampler coupled with an UV/VIS spectrophotometer (UV-2075 Plus detector), from Jasco France (Bouguenais, France)

The HPLC separation column used was a 5 µm Lichrospher 100 RP 18 endcapped column (125 × 4.6 mm ID) (Macherey-Nagel EURL, Hoerd, France)
The HPLC mobile phase was composed of 85/15 phosphate buffer/acetonitrile (v/v) mixture. The phosphate buffer used was a 0.1 mol/L solution of H_2KPO_4 (VWR International Pessac, France). The flow rate through the column for the analysis was set at 1 mL/min, with the column thermo regulated to a temperature of 35°C. The injection volume was of 20 µL. The detection wavelength was set up at 273 nm.

Cefuroxime presents a retention time of 3.8 minutes. This chromatographic method is linear for concentrations ranging from 0.25 µg/mL to 20 µg/mL. The mean linear regression equation obtained is $y = 35022x + 3014.7$ ($r^2 = 0.9998$), where x is the cefuroxime concentration and y the surface area of the corresponding peak. This method has acceptable accuracy and precision as the intra-assay and inter-assay coefficients of variation are below 5%. The limit of quantification of this method is of 0.25 mg/mL.

Cefuroxime release results were expressed in µg of cefuroxime over the loaded surface of anodized TiO_2 (µg/cm^2).

C. Tested parameters

In this work, several parameters that could have an influence on the use of TiO_2 NT as cefuroxime reservoirs were investigated.

1. Influence of the surface nano-topography and loading solution concentration

10 anodized (nano-tubular) non annealed Ti samples, 10 nano-rugged Ti samples, and 10 smooth Ti samples were prepared. 5 samples of each surface nano-topography (15 samples in total) were loaded by immersion into a 150 mg/mL cefuroxime solution, as previously described, whilst the other 5 of each surface nano-topography were loaded with a 25 mg/mL cefuroxime solution.

2. Influence of the nanotube's crystalline structure

To see if annealing (heat treating) the nanotubes could impact their use as cefuroxime carriers as it modifies the nanotubes crystalline structure, annealed nanotubes were compared to non-annealed nanotubes.

7 non-annealed anodized samples and 7 annealed anodized samples were loaded by immersion in a 150 mg/mL cefuroxime solution, as previously described.

D. Statistical considerations

Statistical analysis was performed using a non-parametric Man-Whitney test. The difference was considered significant for a p-value ≤ 0.05.

II. Results

A. Structural characterization and surface wettability

Figure 1 shows the current density time curve for Ti anodization obtained in our operating conditions, and illustrates the nanotube growth. SEM pictures of obtained nano-rugged and nano-tubular samples before loading are presented in Figure 2. Anodization occurred on both sides of the anodized samples.

Nano-smooth non anodized samples typically are not microscopically smooth, but do not present any nano-scale ruggedness. Nano-rugged samples present nano-scale modifications with the formation of what seems to be shallow nanopores, whilst retaining their micro-scale topography. For the 20 minutes anodized samples, the formed nanotubes have dimensions of between 300 to 400 nm high and 70 to 90 nm in diameter.

The XRD results are depicted in Figure 3. The peaks characteristic of anatase and rutile crystalline structure only appear after annealing at 500°C, and are not present in Ti foil or as-anodized Ti .

Concerning the contact angle measurements (data summarised in Table I), anodization times of 80 seconds and 1200 seconds greatly increase the contact angle compared to smooth un-anodized titanium; however the contact angle

measured for an annealed nanotubular surface was lower than un-annealed anodised surface (Figure 4), and even lower than for a nano-smooth surface.

B. Cefuroxime quantification

SEM pictures of loaded samples are shown in Figure 5, with light grey/white colouring showing the titanium sample, and dark grey patches being cefuroxime deposits. In Figure 5(A), a relatively large deposit of cefuroxime can clearly be seen, with Figure 5(B) being a closer view of the phenomenon. Figure 5(C) and Figure 5(D) show how cefuroxime infiltrates and sometimes covers the nano-rugged surface nanopores, and in Figure 5(E) and Figure 5(F) the same can be said of the nano-tubular surface.

Figure 6 (A) and (B) shows the total amount of cefuroxime released over a 90 minutes period from the different tested nano-surfaces with a 25 mg/mL and 150 mg/mL cefuroxime loading solution, and Figure 7 shows the total amount of cefuroxime released over a 90 minutes period for annealed and un-annealed nano-tubular surfaces. Table II summarise the statistical data of the different tested conditions at 90 minutes.

Maximum cefuroxime release for the studied conditions was obtained within the first one or two minutes, and no additional cefuroxime release was detected for the rest of the release study period.

For the nanotube length tested, there is no statistical influence of the nanotube's crystalline structure on the amount of cefuroxime quantified ($p = 0.28$). Cefuroxime loading solution concentration does have a significant impact on cefuroxime quantities released ($p = 0.001$) as does the surface nano-topography, but only between the smooth samples and the nanotube samples for both tested loading solution concentrations ($p = 0.04$). The difference between the nano-rugged surface samples and the nanotubular surface samples is not statistically significant, for

neither loading solution concentrations (p = 0.08). The difference in cefuroxime release is significant between the smooth and nano-rugged surface samples only for a loading solution concentration of 25 mg/mL (p = 0.02).

III. Discussion

The aim of this work was to study several conditions which where hypothesised to influence the use of TiO_2 nanostructures as cefuroxime carriers.

Firstly, to try and characterize whether nanotubes can be used as cefuroxime reservoirs, 3 different nano-topography conditions were compared: smooth, nano-rugged, nano-tubular. After loading, the smooth samples released the least cefuroxime (median 49.89 µg/cm^2), and the nano-tubular samples released the most (median 70.03 µg/cm^2). The difference between the smooth samples and nanotubular samples was statistically different, for both loading solution concentrations, but was much more pronounced for the 25 mg/mL loading solution (4.4-fold increase) when compared to the 150 mg/mL loading solution (40% increase). This could indicate either a loading of the nanotubes (penetration of cefuroxime into the tubes), or an increased surface adsorption, mediated by the nanotubes, or both. It could also be possible the cefuroxime penetrated the interstices visible between the nanotubes. Despite the differences not being significant between the nano-rugged samples and the smooth and nanotubular samples, the quantities of cefuroxime released by the nano-rugged samples are intermediate between the smooth and the nanotubular samples (67.89 µg/cm^2).

There is a statistical difference in released cefuroxime from samples loaded with a 150 mg/mL cefuroxime solution when compared to samples loaded with a 25 mg/mL solution, for all tested surface nano-topographies, which indicates an influence of the loading solution concentration, which is what was expected. However, despite there being a fixed six-fold difference in concentration between the 25 mg/mL and the 150 mg/mL, the obtained difference in quantified cefuroxime was greater, and varied

depending on the nano-topography (24-fold, 20-fold and 7.7-fold for respectively the nano-smooth, nano-rugged and nano-tubular topographies). Such a difference is difficult to explain by just the results' variability. One explanation is that despite a thorough air blowing cleaning procedure, surface adsorption of cefuroxime accounts for an important percentage of total loaded and released drug.

TiO_2 exists naturally in 3 crystalline phases, anatase, rutile and brookite (Roy et al., 2011), yet after their electrochemical formation, TiO_2 nanotubes are amorphous. By annealing (heat treating), the nanotubes can be converted to anatase or rutile, which changes notably the TiO_2 nanotubes electrochemical and photocatalytical properties, but without notably altering the nanotube's morphological characteristics (Lin et al., 2011; Yu and Wang, 2010). In this work, annealed nanotubes did release more cefuroxime than non-annealed, but the difference was not statistically significant, notably due to the observed large variations of cefuroxime release within the annealed group. The annealed nano-tubular surfaces were however much more hydrophilic than the un-annealed nano-tubular surfaces, with a contact angle of 42° versus 120°for the un-anodized nano-tubular. In the conditions of this assay, it is therefore hard to draw any conclusions on the real influence of the crystalline state.

The relatively high cefuroxime quantities quantified with the nano-smooth samples could be linked to moderate surface wettability, as expressed by the measure of water droplet contact angles, as the contact angle for such a surface was measured to be 77°. By contrast, non-annealed anodized surfaces (nano-rugged and nano-tubular) had contact angles measured to be around 120°, expressing a more hydrophobic state, and yet released after loading more cefuroxime. Such results could be in favour of nanotube loading and release of cefuroxime, independently of the surfaces' wettability, at least for the tested conditions.

However, due to the small number of samples, the statistical power of the used test is probably insufficient to identify small differences between certain tested conditions.

In our work, the drug release was nearly immediate, and is much faster than reported in other studies. Popat et al report loaded bovine serum albumin (BSA) and lysozyme using a pipetting method onto unpolished titanium samples with similar TiO_2

nanotubes and obtained maximum release times that varied between 25 and 110 minutes (Popat et al., 2007). Using a similar method, Aninwene et al loaded penicillin/streptomycin or dexamethasone and obtained drug elution for 3 days (Aninwene et al., 2008). The very fast release obtained here could be explained by high Cefuroxime water solubility (150 mg/mL), or by a surface layer of Cefuroxime, or possibly by both. Despite our cleaning method, SEM images showed significant Cefuroxime deposit on the surface of the TiO_2 layer, on samples with different nano-topography, possibly linked to the surface micro-topography. However, since nano-tubular samples released significantly more Cefuroxime than smooth samples, it seems quite plausible that Cefuroxime penetrated at least partially into the nanotubes.

Longer release times have been reported. Peng et al, also using unpolished TiO_2 nanotube surfaces and a consistent cleaning technique, found that elution kinetics of paclitaxel and BSA were influences by nanotube height and pore diameter (Peng et al., 2009), with nanotubes of 5 µm height and 100 nm of diameter releasing the most drug for up to 3 weeks.

Therefore, in this study, the thickness of the nanotube layer could impact the maximum loading capacity of the tubes, as the longer the tube, the more volume it could contain. It could be possible that 400 nm of length is not enough to allow a significant amount of drug into the nanotubes, with regard to the potential surface adsorption. Therefore, any conclusions about the impact of the nanotubes' crystalline structure might be premature, as the 400 nm high nanotubes could have been loaded at maximum capacity regardless of the surface wettability.

In this work, the titanium foil used for the experiments was unpolished, and wasn't microscopically smooth. This could have an impact on cefuroxime adsorption, as SEM structural characterization of samples with different nano-topographies, loaded with cefuroxime, showed an inhomogeneous cefuroxime spread. The microscopic surface features could lead to the formation of "beds" of cefuroxime, protected from the surface cleaning procedure. It has also already been hypothesized that in previous studies at least a significant amount of drug stayed on the surface and did penetrate into the nanotubes (Peng et al., 2009). These microscopic features could also account for the high variability between samples of the same series. Also,

surface adsorption could account for the instant burst-like release that was observed. Therefore, it would seem that in order to more accurately measure the exact quantity of drug actually loaded and then released by the nanotubes, microscopically smooth samples are needed, as well as an adequate and validated surface cleaning method.

Several improvements could be made to this study. To achieve a microscopically smooth surface, a polishing method (electro-chemical polishing or physical polishing) could have been used. The effects of micro-scale ruggedness would therefore be reduced. Also, higher nanotubes could offer improved loading volume and drug storage capacity, and could also improve loading and elution kinetics.

The work presented here seems to indicate that some parameters, like nanotube height and the loading solution concentration, have more influence on cefuroxime release from TiO_2 nanotubes, whereas the crystalline structure of the nanotubes didn't influence the amount of cefuroxime released. The nano-tubular samples released more cefuroxime than nano-smooth or nano-rugged samples, for both 150 mg/mL and 25 mg/mL cefuroxime loading concentrations. However, cefuroxime release kinetics were too fast for lasting local drug delivery, and need to be extended. Longer nanotubes could increase the amount of cefuroxime loaded and release times, but might also increase overall fragility, and thus need to be tested. Also, the antibacterial efficacy of such a delivery method using cefuroxime still needs to be investigated.

IV. Acknowledgements

The authors thank F. Feschet and B. Pereira for their help with the statistical analysis of the data, and C. Massard and V. Raspal for their insights.

V. Bibliography

AlBuhairan, B., Hind, D., Hutchinson, A., 2008. Antibiotic prophylaxis for wound infections in total joint arthroplasty: A SYSTEMATIC REVIEW. J Bone Joint Surg Br 90-B, 915–919.

Aninwene, G.E., Yao, C., Webster, T.J., 2008. Enhanced osteoblast adhesion to drug-coated anodized nanotubular titanium surfaces. Int J Nanomedicine 3, 257–264.

Ayon, A.A., Cantu, M., Chava, K., Agrawal, C.M., Feldman, M.D., Johnson, D., Patel, D., Marton, D., Shi, E., 2006. Drug loading of nanoporous TiO2 films. Biomed Mater 1, L11–15.

Campoccia, D., Montanaro, L., Arciola, C.R., 2006. The significance of infection related to orthopedic devices and issues of antibiotic resistance. Biomaterials 27, 2331–2339.

Cuckler, J.M., 2005. The Infected Total Knee: Management Options. The Journal of Arthroplasty 20, Supplement 2, 33–36.

Dale, H., Skråmm, I., Løwer, H.L., Eriksen, H.M., Espehaug, B., Furnes, O., Skjeldestad, F.E., Havelin, L.I., Engesaeter, L.B., 2011. Infection after primary hip arthroplasty: a comparison of 3 Norwegian health registers. Acta Orthop 82, 646–654.

Ghicov, Andrei, Schmuki, Patrik, 2009. Self-ordering electrochemistry: a review on growth and functionality of TiO2 nanotubes and other self-aligned MOx structures. Chem. Commun. 2791–2808.

Gillespie, W.J., Walenkamp, G.H., 1996. Antibiotic prophylaxis for surgery for proximal femoral and other closed long bone fractures, in: Cochrane Database of Systematic Reviews. John Wiley & Sons, Ltd.

Gulati, K., Aw, M.S., Losic, D., 2011. Drug-eluting Ti wires with titania nanotube arrays for bone fixation and reduced bone infection. Nanoscale Research Letters 6, 571.

Iorio, R., Robb, W.J., Healy, W.L., Berry, D.J., Hozack, W.J., Kyle, R.F., Lewallen, D.G., Trousdale, R.T., Jiranek, W.A., Stamos, V.P., Parsley, B.S., 2008. Orthopaedic Surgeon Workforce and Volume Assessment for Total Hip and Knee Replacement in the United States: Preparing for an Epidemic. J Bone Joint Surg Am 90, 1598–1605.

Jämsen, E., Varonen, M., Huhtala, H., Lehto, M.U.K., Lumio, J., Konttinen, Y.T., Moilanen, T., 2010. Incidence of prosthetic joint infections after primary knee arthroplasty. J Arthroplasty 25, 87–92.

Kang, H.-J., Kim, D.J., Park, S.-J., Yoo, J.-B., Ryu, Y.S., 2007. Controlled drug release using nanoporous anodic aluminum oxide on stent. Thin Solid Films 515, 5184–5187.

Kim, D., Macak, Jan M, Schimidt-Stein, F., Schmuki, Patrik, 2008. Capillary effects, wetting behavior and photo-induced tube filling of TiO2 nanotube layers. Nanotechnology 19, 305710.

Kuong, E.E., Ng, F.Y., Yan, C.H., Fang, C.X.S., Chiu, P.K.Y., 2009. Antibiotic prophylaxis after total joint replacements. Hong Kong Med J 15, 458–462.

Kurtz, S., Ong, K., Lau, E., Mowat, F., Halpern, M., 2007. Projections of primary and revision hip and knee arthroplasty in the United States from 2005 to 2030. J Bone Joint Surg Am 89, 780–785.

Lin, J.Y., Chou, Y.T., Shen, J.L., Yang, M.D., Wu, C.H., Chi, G.C., Chou, W.C., Ko, C.H., 2011. Effects of rapid thermal annealing on the structural properties of TiO2 nanotubes. Applied Surface Science 258, 530–534.

Losic, D., Simovic, S., 2009. Self-ordered nanopore and nanotube platforms for drug delivery applications. Expert Opinion on Drug Delivery 6, 1363–1381.

Macak, J.M., Tsuchiya, H., Ghicov, A., Yasuda, K., Hahn, R., Bauer, S., Schmuki, P., 2007. TiO2 nanotubes: Self-organized electrochemical formation, properties and applications. Current Opinion in Solid State and Materials Science 11, 3–18.

Meehan, J., Jamali, A.A., Nguyen, H., 2009. Prophylactic Antibiotics in Hip and Knee Arthroplasty. JBJS 91, 2480–2490.

Memtsoudis, S.G., Pumberger, M., Ma, Y., Chiu, Y.-L., Fritsch, G., Gerner, P., Poultsides, L., Valle, A.G.D., 2012. Epidemiology and risk factors for perioperative mortality after total hip and knee arthroplasty. Journal of Orthopaedic Research 30, 1811–1821.

Montanaro, L., Speziale, P., Campoccia, D., Ravaioli, S., Cangini, I., Pietrocola, G., Giannini, S., Arciola, C.R., 2011. Scenery of Staphylococcus implant infections in orthopedics. Future Microbiology 6, 1329–1349.

Ong, K.L., Kurtz, S.M., Lau, E., Bozic, K.J., Berry, D.J., Parvizi, J., 2009. Prosthetic joint infection risk after total hip arthroplasty in the Medicare population. J Arthroplasty 24, 105–109.

Peng, L., Mendelsohn, A.D., LaTempa, T.J., Yoriya, S., Grimes, C.A., Desai, T.A., 2009. Long-Term Small Molecule and Protein Elution from TiO2 Nanotubes. Nano Lett. 9, 1932–1936.

Phillips, J.E., 2006. The incidence of deep prosthetic infections in a specialist orthopaedic hospital: A 15-YEAR PROSPECTIVE SURVEY. Journal of Bone and Joint Surgery - British Volume 88-B, 943–948.

Popat, K.C., Eltgroth, M., LaTempa, T.J., Grimes, C.A., Desai, T.A., 2007. Titania Nanotubes: A Novel Platform for Drug-Eluting Coatings for Medical Implants? Small 3, 1878–1881.

Pulido, L., Ghanem, E., Joshi, A., Purtill, J.J., Parvizi, J., 2008. Periprosthetic joint infection: the incidence, timing, and predisposing factors. Clin. Orthop. Relat. Res. 466, 1710–1715.

Roy, P., Berger, S., Schmuki, Patrik, Roy, P., Berger, S., Schmuki, Patrik, 2011. TiO2 Nanotubes: Synthesis and Applications, TiO2 Nanotubes: Synthesis and Applications. Angewandte Chemie International Edition 50, 2904–2939.

Schmidmaier, G., Lucke, M., Wildemann, B., Haas, N.P., Raschke, M., 2006. Prophylaxis and treatment of implant-related infections by antibiotic-coated implants: a review. Injury 37, S105–S112.

Senthi, S., Munro, J., Pitto, R., 2011. Infection in total hip replacement: meta-analysis. International Orthopaedics 35, 253–260.

Smilack, J.D., Flittie, W.H., Williams, T.W., Jr, 1976. Bone concentrations of antimicrobial agents after parenteral administration. Antimicrob. Agents Chemother. 9, 169–171.

Société de Pathologie Infectieuse de Langue Française (SPILF), 2009. Recommandations de pratique clinique: Infections ostéo-articulaires sur matériel (prothèse, implant, ostéo-synthèse) - Mai 2009 - 107 pages.

Société française d'anesthésie et de réanimation, 2011. Antibioprophylaxie en chirurgie et médecine interventionnelle (patients adultes). Actualisation 2010. Annales Françaises d'Anesthésie et de Réanimation 30, 168–190.

Yu, J., Wang, B., 2010. Effect of calcination temperature on morphology and photoelectrochemical properties of anodized titanium dioxide nanotube arrays. Applied Catalysis B: Environmental 94, 295–302.

Zilberman, M., Elsner, J.J., 2008. Antibiotic-eluting medical devices for various applications. J Control Release 130, 202–215.

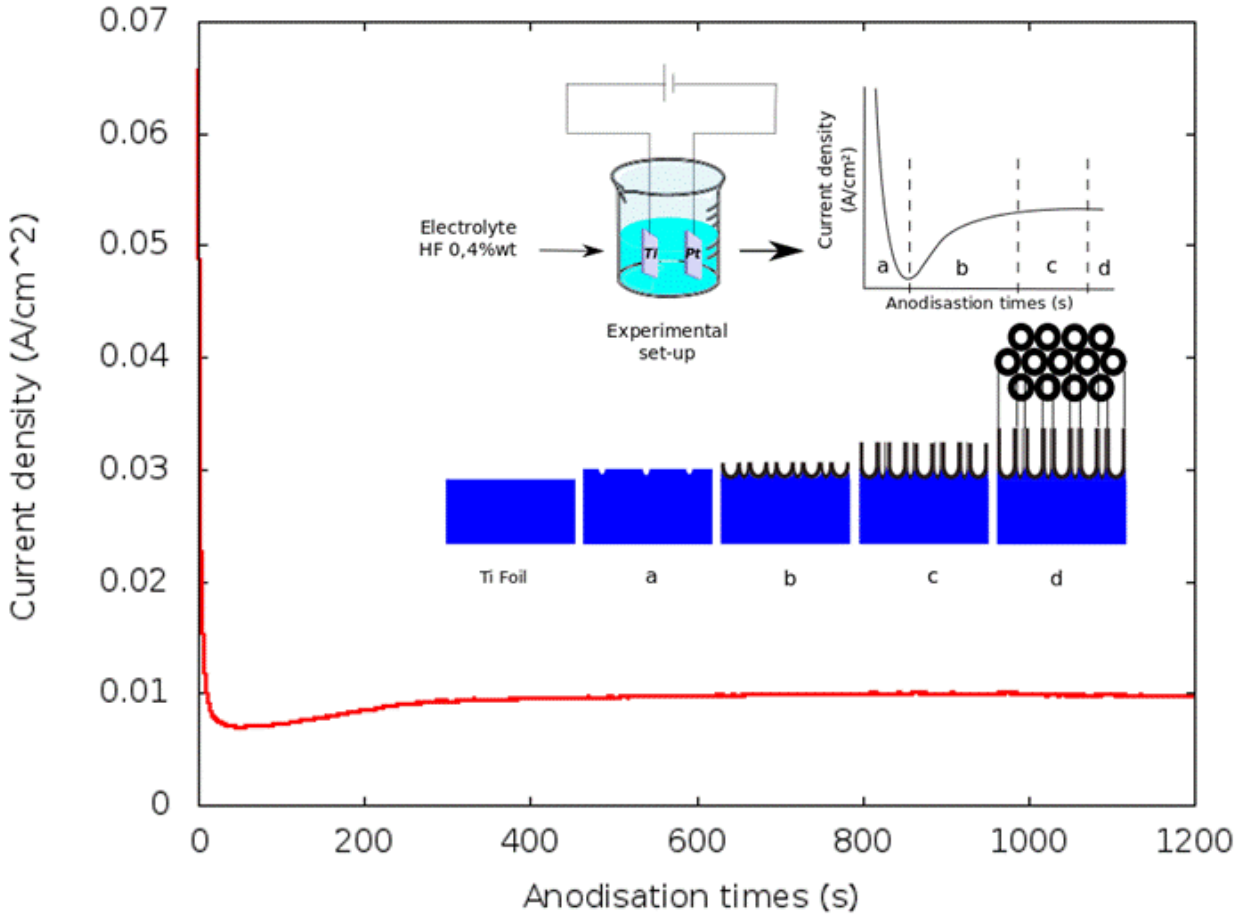

Figure 1: Current density time curve with experimental setup. Nanotubes appear to be fully formed as of 20 minutes (1200 seconds) of anodizing time (d). The nano-rugged surface was obtained with an anodizing time of 80 seconds, which corresponds to the low point of current density curve, between stage (a) and (b).

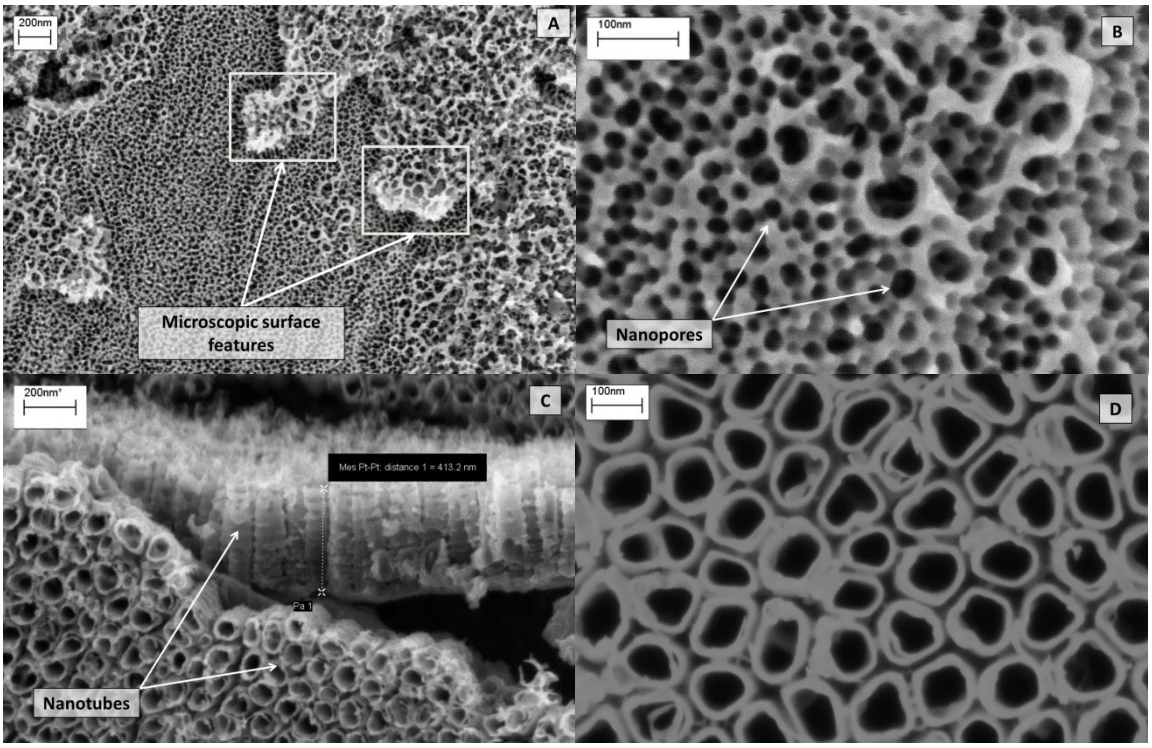

Figure 2 (A), (B), (C) and (D): Surface topography of a nano-rugged (A) and (B) and nano-tubular (C) and (D) anodized TiO_2 sample by SEM, before loading.

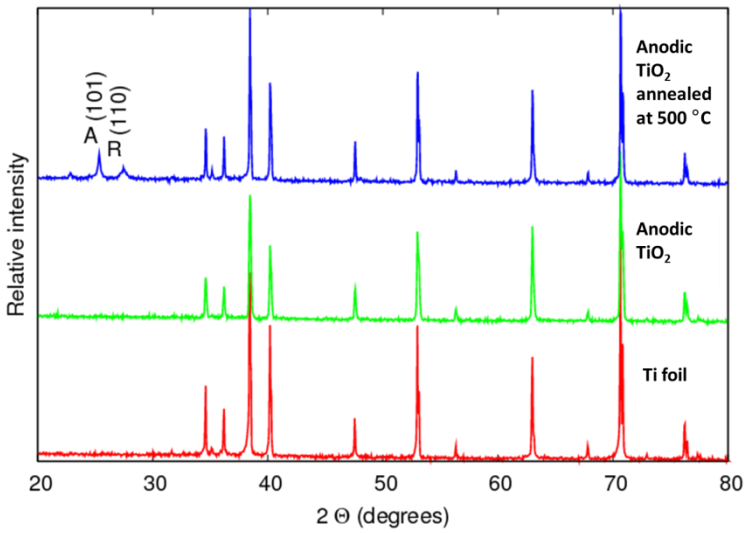

Figure 3: X-ray diffractogram of smooth Ti foil (bottom graph), anodized (Anodic TiO2, middle graph) and 500°C annealed anodized titanium foil (top graph) with two peaks (A and R) corresponding to respectively the anatase and rutile crystalline phase.

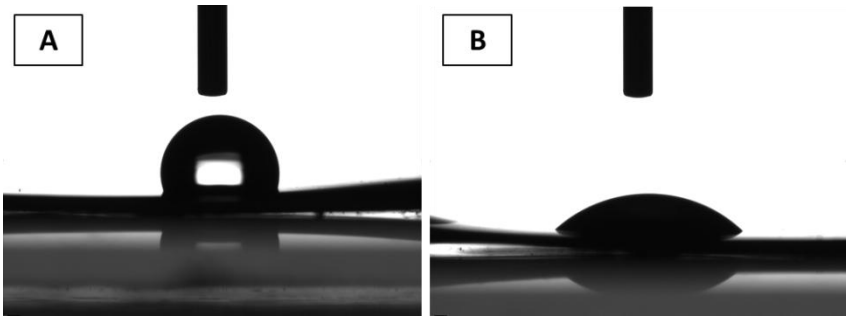

Figure 4: (A) un-annealed nano-tubular sample and (B) annealed nano-tubular sample

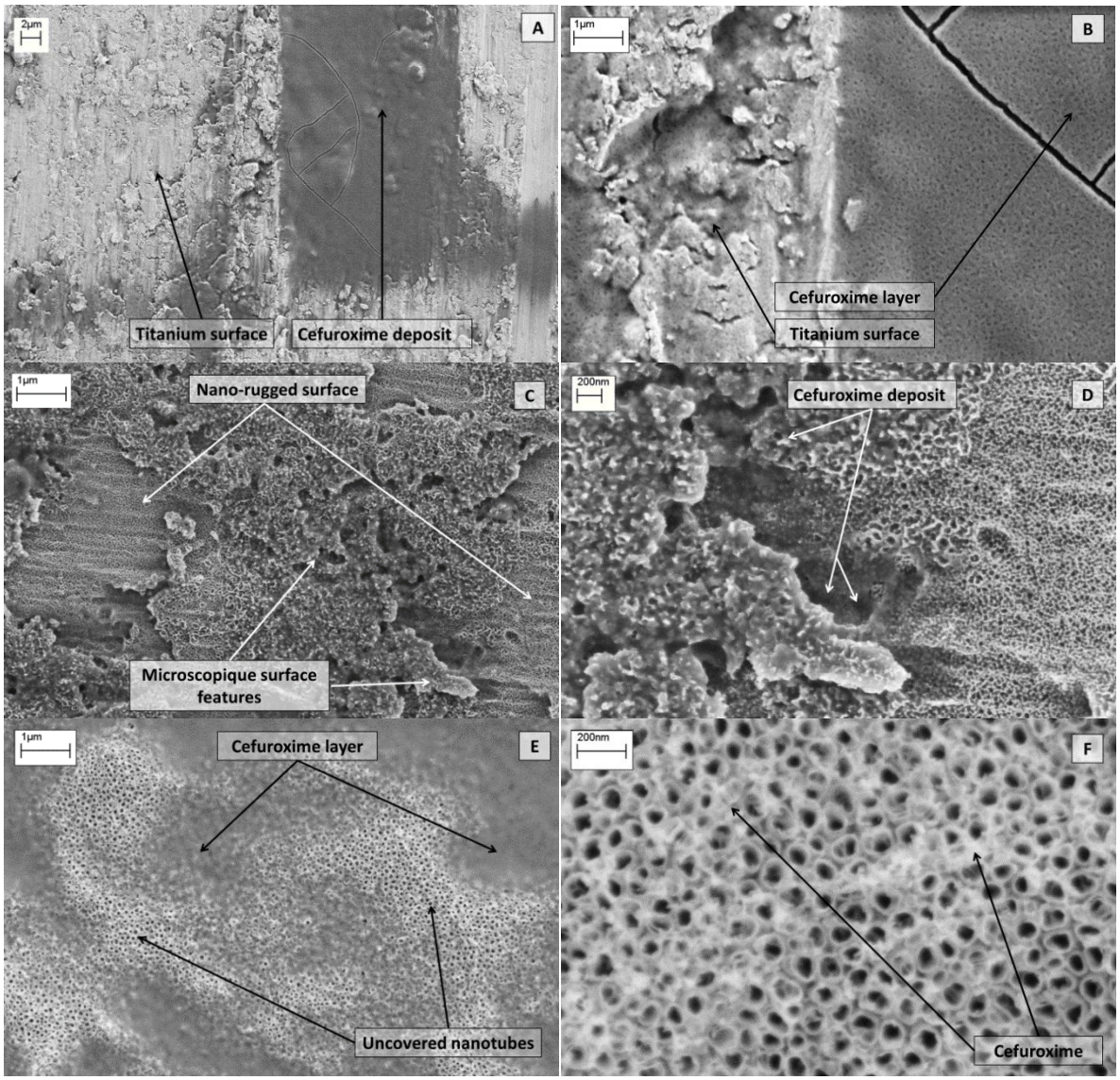

Figure 5: (A) and (B): smooth titanium sample after cefuroxime loading, with (B) being a close up view of (A). (C) and (D): nano-rugged titanium sample with cefuroxime deposit and infiltration in the surface nanopores, with (D) being a close up view of (C). (E) and (F): nano-tubular titanium sample with cefuroxime deposit and infiltration in the surface nanopores.

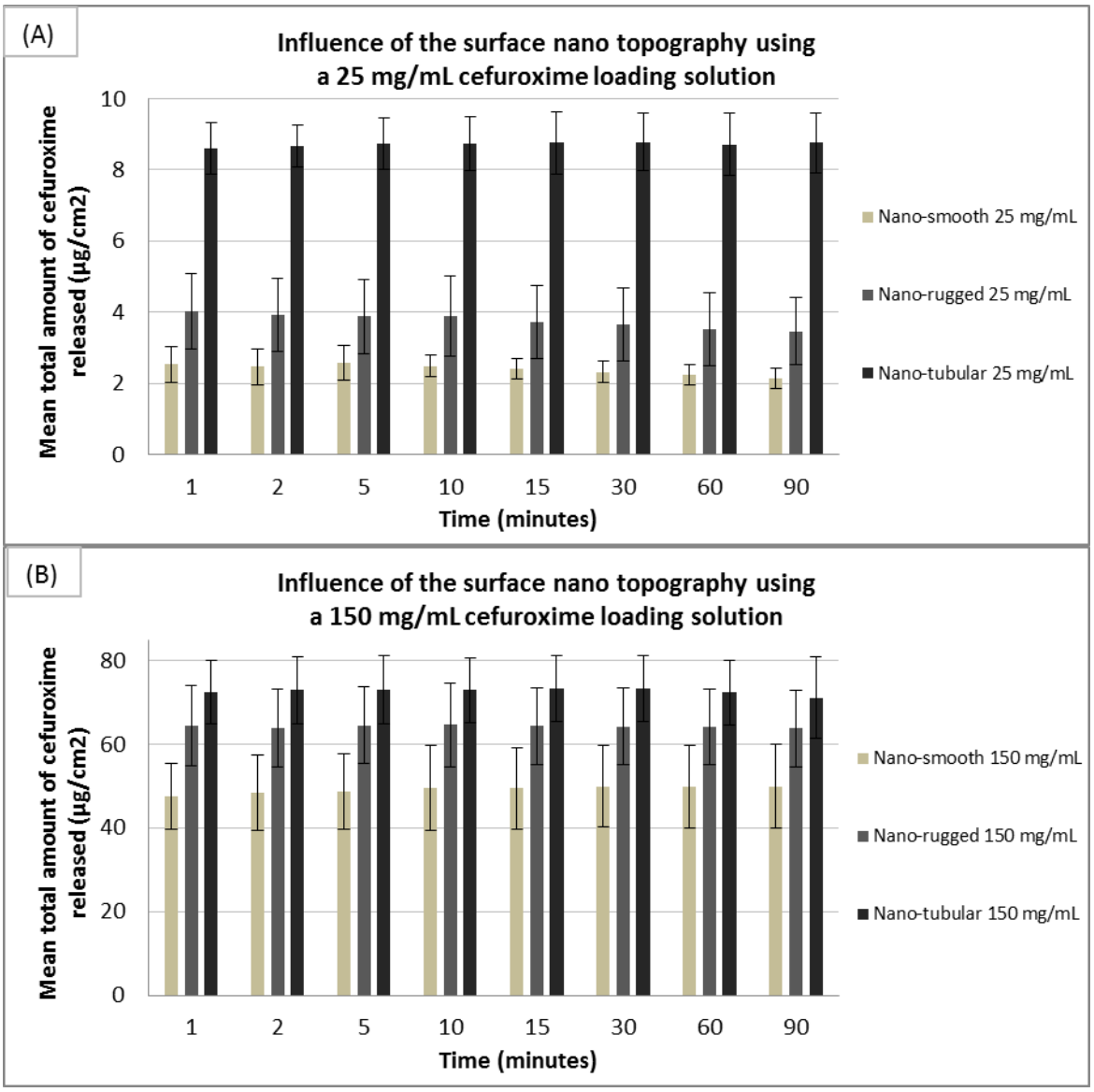

514

515 Figure 6: Total amount of released cefuroxime during 90 minutes for the different
516 tested nano-topography and cefuroxime loading solution conditions

517

518

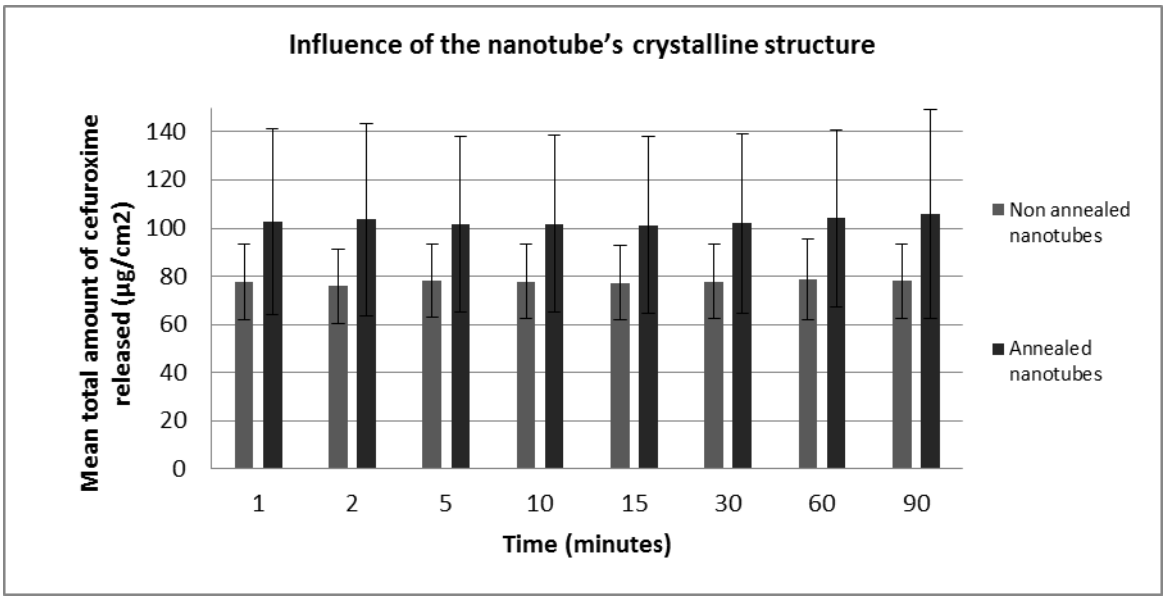

Figure 7: Total amount of cefuroxime released during 90 minutes for amorphous and crystalline structures

Table I : Contact angle measurement data

Measured contact angle	Mean contact angle	Confidence intervalle 95%
Nano-smooth surface	77,18	1,90
Non-annealed nano-rugged surface	122,00	1,95
Non-annealed nano-tubular surface	118,00	0,72
Annealed nano-tubular surface	41,73	0,67

Table II : Statistical data for the different tested conditions at 90 minutes

Cefuroxime release at t = 90 minutes		Number of samples	Median total quantity of Cefuroxime (µg/cm^2)	Interquartile range	Mean total quantity of Cefuroxime (µg/cm^2)	Standard deviation	Variation coefficient (%)
Surface nano-topography and Loading solution concentration	25 mg/mL nano-smooth	3	2,07	0,55	2,13	0,28	13,2
	25 mg/mL nano-rugged	4	3,45	1,22	3,46	0,95	27,4
	25 mg/mL nano-tubular	4	9,09	1,58	8,77	0,84	9,6
	150 mg/mL nano-smooth	4	49,89	15,61	50,00	10,06	20,1
	150 mg/mL nano-rugged	4	67,89	17,84	63,86	9,07	14,2
	150 mg/mL nano-tubular	4	70,03	10,38	71,17	9,75	13,7
Crystalline structure	Non annealed	7	76,99	21,76	78,11	15,40	19,7
	Annealed	7	87,28	72,21	105,90	43,44	41,0

530